

# Accepted Manuscript

Research papers

Groundwater Flux Estimation in Streams: A Thermal Equilibrium Approach

Yan Zhou, Garey A. Fox, Ron B. Miller, Robert Mollenhauer, Shannon Brewer

PII: S0022-1694(18)30243-9

DOI: <https://doi.org/10.1016/j.jhydrol.2018.04.001>

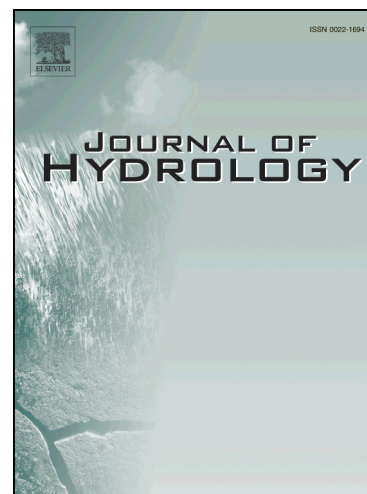
Reference: HYDROL 22704

To appear in: *Journal of Hydrology*

Received Date: 25 January 2018

Revised Date: 28 March 2018

Accepted Date: 1 April 2018



Please cite this article as: Zhou, Y., Fox, G.A., Miller, R.B., Mollenhauer, R., Brewer, S., Groundwater Flux Estimation in Streams: A Thermal Equilibrium Approach, *Journal of Hydrology* (2018), doi: <https://doi.org/10.1016/j.jhydrol.2018.04.001>

This is a PDF file of an unedited manuscript that has been accepted for publication. As a service to our customers we are providing this early version of the manuscript. The manuscript will undergo copyediting, typesetting, and review of the resulting proof before it is published in its final form. Please note that during the production process errors may be discovered which could affect the content, and all legal disclaimers that apply to the journal pertain.

1           **Groundwater Flux Estimation in Streams: A Thermal Equilibrium Approach**

2  
3           Yan Zhou, Garey A. Fox\*, Ron B. Miller, Robert Mollenhauer, Shannon Brewer

4  
5           Yan Zhou, Ph.D., and Ron Miller, Ph.D., Department of Biosystems and Agricultural  
6 Engineering, Oklahoma State University, Stillwater, OK; G. A. Fox\*, Department of Biological  
7 and Agricultural Engineering, North Carolina State University, Raleigh, NC; Robert  
8 Mollenhauer, Ph.D., and Shannon Brewer, Ph.D., U.S. Geological Survey, Oklahoma  
9           Cooperative Fish and Wildlife Research Unit, Stillwater, OK.

10  
11           \*Corresponding author: Dr. Garey A. Fox, Professor and Department Head, Department of  
12 Biological and Agricultural Engineering, North Carolina State University, Campus Box 7625,  
13           Raleigh, NC 27695, Phone: 919-515-6700; E-mail: [garey\\_fox@ncsu.edu](mailto:garey_fox@ncsu.edu).

14  
15           Abbreviations: NSE, Nash–Sutcliffe Efficiency coefficient; RMSE, root mean square error; TEM,  
16           thermal equilibrium method; WASP, Water Quality Analysis Simulation Program

18 **Groundwater Flux Estimation in Streams: A Thermal Equilibrium Approach**

19 **Abstract.** Stream and groundwater interactions play an essential role in regulating flow,  
20 temperature, and water quality for stream ecosystems. Temperature gradients have been used to  
21 quantify vertical water movement in the streambed since the 1960s, but advancements in thermal  
22 methods are still possible. Seepage runs are a method commonly used to quantify exchange rates  
23 through a series of streamflow measurements but can be labor and time intensive. The objective  
24 of this study was to develop and evaluate a thermal equilibrium method as a technique for  
25 quantifying groundwater flux using monitored stream water temperature at a single point and  
26 readily available hydrological and atmospheric data. Our primary assumption was that stream  
27 water temperature at the monitored point was at thermal equilibrium with the combination of all  
28 heat transfer processes, including mixing with groundwater. By expanding the monitored stream  
29 point into a hypothetical, horizontal one-dimensional thermal modeling domain, we were able to  
30 simulate the thermal equilibrium achieved with known atmospheric variables at the point and  
31 quantify unknown groundwater flux by calibrating the model to the resulting temperature  
32 signature. Stream water temperatures were monitored at single points at nine streams in the  
33 Ozark Highland ecoregion and five reaches of the Kiamichi River to estimate groundwater fluxes  
34 using the thermal equilibrium method. When validated by comparison with seepage runs  
35 performed at the same time and reach, estimates from the two methods agreed with each other  
36 with an  $R^2$  of 0.94, a root mean squared error (RMSE) of 0.08 (m/d) and a Nash–Sutcliffe  
37 efficiency (NSE) of 0.93. In conclusion, the thermal equilibrium method was a suitable technique  
38 for quantifying groundwater flux with minimal cost and simple field installation given that  
39 suitable atmospheric and hydrological data were readily available.

40 **Keywords.** Groundwater flux; Thermal equilibrium; Seepage run; Stream water temperature;  
41 Temperature signature

42

### 43 **Introduction**

44 The interaction of stream water with groundwater influences water quality and quantity  
45 and plays an essential role in aquatic ecosystems. Streams with high groundwater interactions are  
46 often characterized by high biological and microbial diversity and activity due to elevated solute  
47 transport and nutrient exchange across the streambed interface (Laursen and Seitzinger, 2005;  
48 Schmidt et al., 2007). Groundwater flux can also limit benthic invertebrate exposure to low  
49 oxygen and contaminants (Malard and Hervant, 1999), and provide thermal refugia and  
50 microbial food supply for fishes (e.g., salmon) (Kurylyk et al., 2013). The importance of  
51 groundwater to stream biota has led to increased efforts to quantify the effects of groundwater on  
52 both stream temperatures (Constantz, 1998) and energy sources (Barlocher and Murdoch, 1989).  
53 However, the complex nature of stream-groundwater hydrological connectivity can make  
54 quantifying those interactions difficult and labor intensive.

55 Over the past few decades, many approaches have been developed to quantify stream and  
56 groundwater interactions that can be generally categorized into Darcian, streamflow, water  
57 budget and tracer methods (Table 1). Extensive reviews of these approaches have been provided  
58 by Kalbus et al. (2006), Brodie et al. (2007), and Turner (2009), but are briefly overviewed  
59 below. Darcian methods calculate point stream-groundwater exchange flux as the product of  
60 measured hydraulic gradient and conductivity based on Darcy's Law in a manner similar to that  
61 used to investigate water movement in porous media (Freeze and Cherry, 1979). Water budget  
62 methods use groundwater and watershed models, separately or in combination, to estimate

63 groundwater and stream interactions as the unknown residual of the water budget by calibrating  
64 the model against streamflow records and estimated physical parameters of the aquifer.

65 Streamflow methods include a variety of approaches such as hydrograph separation,  
66 direct measurement using seepage meters and seepage runs (Harvey and Wagner, 2000). The  
67 hydrograph separation methods, such as recession-curve displacement and stream base-flow  
68 analysis, use various assumptions to separate a stream hydrograph into the different runoff,  
69 interflow, and baseflow components (Scanlon et al., 2002). The seepage meter method allows  
70 direct point measurement of stream and groundwater flux by calculating the rate of volume  
71 change of a collection bag over the area of the collecting bucket pushed into the streambed  
72 (Zamora, 2008). The incremental streamflow method for estimating groundwater flux (hereafter  
73 ‘seepage run’) involves measuring streamflow at multiple transects along the river (Donato, 1998;  
74 Harvey and Wagner, 2000). After eliminating contributions from tributaries, the surface-  
75 groundwater flux is assumed to be the flow rate difference between transects (Rosenberry and  
76 LaBaugh, 2008). Tracer methods estimate groundwater flux based on the mass balance of tracers.  
77 Introduced tracers, commonly chloride or dyes, are usually used in either dilution gauging or  
78 transient storage approaches (Zhou et al., 2016) while environmental tracers such as tritium and  
79 chlorofluorocarbons are used in hydrograph separation to provide information on groundwater  
80 flux. The limitations of these conventional methods are the high time and material cost for proper  
81 installation and maintenance (e.g., Darcian method with piezometer and seepage meter) (Berry et  
82 al., 2011) and the difficulty in parameter estimation (e.g., water budget methods) (Scanlon et al.,  
83 2002). Due to the ease of monitoring stream temperatures, thermal methods overcome some of  
84 these limitations and have gained increasing popularity in recent decades (Webb et al., 2008).

85 Thermal methods use heat as an environmental tracer with the analysis based on heat  
86 transfer and energy balance analogous to the mass balance of common chemical tracers. Thermal  
87 methods emerged as a versatile class of geophysical tools for monitoring focused recharge in arid  
88 and semiarid settings, but did not come into common use until the 1960s (Blasch et al., 2007)  
89 after analytical solutions to the coupled heat and water transport equations were established by  
90 Suzuki (1960), Stallman (1965), and Bredehoeft and Papaopulos (1965). The vertical thermal  
91 gradient method exploits the coupled relationship between heat and water advection and  
92 conduction processes to model vertical heat and water movement across the streambed  
93 (Anderson, 2005). By monitoring the temperature of stream water and saturated bed sediment at  
94 multiple depths over time, this method estimates the vertical movement of groundwater. This  
95 method has been used to investigate infiltration and percolation on the land surface (Suzuki,  
96 1960), indicate gaining and losing reaches of stream channels (Lapham, 1989; Silliman and  
97 Booth, 1993; Constantz, 1998), and locate areas of inflow to lakes (Lee, 1985).

98 The stream thermal modeling approach typically uses a process-based model (Becker et  
99 al., 2004; Loheide and Gorelick, 2006) to simulate the heat budget of the stream using known  
100 hydrological and atmospheric variables and quantify heat introduced by groundwater flux as the  
101 residual of the known stream water heat budget. For example, Sinokrot and Stefan (1993)  
102 developed a numerical, finite-difference model for stream temperatures. In shallow streams, they  
103 noted the primary importance of incoming solar radiation but that other components of the heat  
104 balance (long-wave back radiation, evaporation, convection to the atmosphere, and conductive  
105 heat exchange between the streambed and water) are also significant. In an attempt to develop a  
106 tool for ecohydrological assessment in a watershed, Loinaz et al. (2013) applied a surface water-  
107 groundwater flow and heat transport model to predict stream temperatures. They noted the

108 importance of spatially distributed flow dynamics for calibrating the model to match stream  
109 temperatures. A benefit of stream temperature modeling is that it can be performed at small  
110 spatial and temporal resolutions. For example, Westhoff et al. (2007) used data from a  
111 distributed temperature sensing system with 1.0 m spatial and two-minute temporal resolution to  
112 model stream temperature. Their results suggested that lateral groundwater inflow was a  
113 significant parameter for numerically predicting stream temperatures.

114         Despite these advances, there are still new potential applications for thermal methods.  
115 The vertical thermal gradient method provides a convenient alternative for quantifying  
116 groundwater flux at point scales, but the material and time costs are significant if the scale is to  
117 be expanded using multiple measurements. Stream thermal modeling methods estimate  
118 groundwater flux at a larger scale with relatively lower cost, but it loses the sensitivity of point  
119 estimations. Thus, there is still a need for accurate, convenient, and economical means of  
120 quantifying point groundwater flux that can be expanded to cover a predetermined area, e.g.,  
121 stream reach.

122         This research proposed a thermal equilibrium method (hereafter TEM) to estimate the  
123 time-averaged groundwater flux to a stream using monitored stream water temperature data at a  
124 single point and atmospheric and hydrological data. The proposed approach significantly reduces  
125 the need and cost of data collection while maintaining the sensitivity and independence of a point  
126 measurement. The research validated the performance of the TEM by comparison with estimates  
127 from seepage runs (i.e., streamflow measurements).

## 128 **Materials and Methods**

### 129 *Thermal Equilibrium Method*

130 The TEM was developed based on the assumed thermal equilibrium of all heat transfer  
131 processes in the stream including both atmospheric heat transfer and groundwater interactions.  
132 Equilibrium stream water temperature, calculated based on atmospheric conditions (atmospheric  
133 equilibrium water temperature, hereafter  $T_{AE}$ ), has traditionally been used as an approximation to  
134 stream water temperature (hereafter  $T_S$ ) (Smith, 1981). Recent research showed that the  $T_{AE}$   
135 calculated on a weekly or coarser temporal scale was linearly related, but not equal to  $T_S$  (Bogan  
136 et al., 2003). The differences between  $T_{AE}$  and  $T_S$  were attributed to external water inputs,  
137 primarily groundwater interactions for 80% of 596 sites in the eastern and central USA (Bogan et  
138 al., 2003; Bogan et al., 2004; Webb et al., 2008). In the current study, we assumed that by  
139 including groundwater interactions, a more comprehensive equilibrium water temperature  
140 (hereafter  $T_E$ ) could be calculated to appropriately represent  $T_S$  on a weekly or coarser temporal  
141 scale. In another words, we assumed streams were at thermal equilibrium with the combination  
142 of atmospheric conditions and groundwater interactions.

143 A stream temperature model was applied to simulate the atmospheric heat transfer  
144 processes (i.e., heat conduction, shortwave solar radiation, longwave atmospheric radiation, etc.)  
145 based on the upstream boundary of monitored  $T_S$  and atmospheric and hydrological conditions of  
146 the monitored point. The monitored stream point was represented by an expanded continuous  
147 model domain (Figure 1), allowing the model to stabilize and predict  $T_{AE}$  at the downstream  
148 boundary. Based on the thermal equilibrium assumption, the difference between  $T_S$  (upstream  
149 boundary) and predicted  $T_{AE}$  (downstream boundary) was attributed to groundwater flux.  
150 Therefore, if the predicted  $T_{AE}$  of the downstream boundary differed from the upstream  $T_S$ , a  
151 groundwater flux could be applied to the domain and calibrated until the difference between the

152 two boundaries was minimized ( $T_E = T_S$ ). The magnitude of the flux required for thermal  
 153 equilibrium would provide an estimate of the unknown groundwater flux at the monitoring point.

154 In this study, the Water Quality Analysis Simulation Program (WASP) was used to  
 155 simulate stream heat transfer with an output temporal resolution of 1 hr. WASP, developed by  
 156 the U.S. Environmental Protection Agency (EPA) (Wool et al., 2006), is a dynamic  
 157 compartment-modeling program for pollutant transport in aquatic systems. The time-varying  
 158 processes of advection, dispersion, point and diffuse mass loading and boundary exchange are  
 159 represented in the basic program. In the WASP temperature module, heat transfer is computed  
 160 based on the following one-dimensional advection-diffusion equation:

$$161 \quad \frac{\partial T_s}{\partial t} = -\frac{\partial}{\partial x}(V_x T_s) + \frac{\partial}{\partial x}\left(D_x \frac{\partial T_s}{\partial x}\right) + \frac{H_n A_s}{\rho_w C_p V} + S \quad (1)$$

162 where  $T_s$  is the stream water temperature ( $^{\circ}\text{C}$ ),  $V_x$  is the advective velocity (m/s),  $D_x$  is the  
 163 dispersion coefficient ( $\text{m}^2/\text{s}$ ),  $V$  is the segment volume ( $\text{m}^3$ ),  $A_s$  is the segment surface area ( $\text{m}^2$ ),  
 164  $\rho_w$  is the density of water ( $997 \text{ kg}/\text{m}^3$ ),  $C_p$  is the specific heat of water ( $4179 \text{ J}/\text{kg } ^{\circ}\text{C}$ ),  $H_n$  is the  
 165 net surface heat flux ( $\text{W}/\text{m}^2$ ), and  $S$  is the loading rate include boundary, direct and diffuse  
 166 loading ( $^{\circ}\text{C}/\text{s}$ ). The net surface heat flux includes the effects of a number of processes computed  
 167 as (Cole and Buchak, 1995):

$$168 \quad H_n = H_s + H_a + H_e + H_c - (H_{sr} + H_{ar} + H_{br}) \quad (2)$$

169 where  $H_n$  is the net heat flux across the water surface ( $\text{W}/\text{m}^2$ ),  $H_s$  is the incident short wave solar  
 170 radiation ( $\text{W}/\text{m}^2$ ),  $H_a$  is the incident long wave atmospheric radiation ( $\text{W}/\text{m}^2$ ),  $H_{sr}$  is the reflected  
 171 short wave solar radiation ( $\text{W}/\text{m}^2$ ),  $H_{ar}$  is the reflected long wave radiation ( $\text{W}/\text{m}^2$ ),  $H_{br}$  is the  
 172 back radiation from the water surface ( $\text{W}/\text{m}^2$ ),  $H_e$  is the evaporative heat loss ( $\text{W}/\text{m}^2$ ), and  $H_c$  is  
 173 the heat conduction ( $\text{W}/\text{m}^2$ ).

174 In this study, a one-dimensional conceptual domain with a length of 2 km was  
175 constructed in WASP and divided into twenty 100 m-long segments (Figure 2). A monitored  $T_S$   
176 time series was input as the upstream boundary and the initial temperature for each segment was  
177 set to the  $T_S$  at the first time step. The geometry and flow rate in the main channel of the model  
178 were assumed to be uniform and described by parameters acquired from transect measurements  
179 at the monitored point (see seepage runs below). An atmospheric time series was obtained from  
180 the nearest Oklahoma Mesonet station and input into the WASP model to compute heat transfer  
181 at each time step. The Oklahoma Mesonet includes 121 automated weather-monitoring stations  
182 distributed throughout Oklahoma with observations every 5 minutes (<http://mesonet.org>, Brock  
183 et al., 1995). The effect of canopy cover was neglected because the studied reaches were located  
184 on unshaded areas of higher order streams. Thermal interaction of groundwater flux was  
185 represented by a uniform flow input across the twenty segments and incorporated in the model  
186 via hydrological connections (Figure 2).

187 Using measured or estimated groundwater temperature, atmospheric and hydrologic  
188 variables, estimates for thermal variables such as the dispersion coefficient, and constants for  
189 thermal properties, the approach then calibrates the magnitude of the groundwater flux until the  
190 sum of squared error (SSE) was minimized between the predicted  $T_E$  at the downstream  
191 boundary and  $T_S$  at the upstream boundary. When the temperature at the two boundaries matched,  
192 the net heat transfer across the conceptual domain was zero and all the heat transfer processes  
193 were equilibrated. The estimated flow represented the optimal groundwater flux required for the  
194  $T_S$  to equilibrate as indicated in the thermal equilibrium assumption.

195 In this study, the groundwater temperature time series was estimated from air temperature  
196 with a 1.5-month time lag as recommended by Pluhowski (1970) (Figure 3). The air temperature

197 offset assumed in this research allows easy application of the TEM. Alternatively, practitioners  
198 can measure or estimate GW temperatures using a method of their choice and utilize those data  
199 in the TEM methodology. Measuring local groundwater temperatures can allow the  
200 consideration of more local conditions. Also, note that the length and number of segments  
201 constructed in the model did not physically represent the monitored point, but served only as a  
202 model domain that allowed the model to stabilize.

### 203 *Study Areas*

204 To validate the TEM by comparison with seepage runs (i.e., streamflow measurements),  
205 five sampling reaches were chosen on the Kiamichi River (Figure 4). The Kiamichi River  
206 watershed in southeast Oklahoma has an area of about 4800 km<sup>2</sup>, with elevation ranging from  
207 270 to 810 m (Pyron et al., 1998). The sedimentary rocks of the area have been deformed into  
208 tightly folding anticlines and synclines forming steep east-west trending ridges separated by a  
209 broad and flat-bottomed stream valley. The area was expected to have substantial groundwater  
210 storage potential as well as permeability to allow stream and groundwater interactions.

211 Nine additional sampling reaches were located on different streams in the Springfield  
212 Plateau in the Ozark Highland ecoregion of Missouri, Arkansas and Oklahoma (Figure 4). The  
213 Springfield Plateau comprises the southwest portion of the Ozark Plateau with an area of  
214 approximately 26,700 km<sup>2</sup> including parts of west-central and southwest Missouri, northeast  
215 Oklahoma, southeast Kansas and northern Arkansas (Adamski et al., 1995). Elevations range  
216 from 300 to 520 m with mostly gentle topographic relief except for Eureka Springs Escarpment  
217 that separates the Springfield and Salem Plateaus. Most streams in Springfield Plateau drain  
218 radially from the plateau center (Adamski et al., 1995; Nigh and Schroeder, 2002). The limestone  
219 bedrock in the region is intermittently soluble, producing regionally abundant sinkholes, springs,

220 and caves (Nigh and Schroeder, 2002). The Springfield Plateau overlies the Ozark Plateau  
221 aquifer system, which extends throughout southern Missouri, eastern Oklahoma, southeast  
222 Kansas and a large area of northwest Arkansas (Miller and Appel, 1997). Extending sites to the  
223 Ozark Highlands allowed us to test the TEM on streams with higher expected groundwater  
224 contributions due to the predominant karst topography. All of the study sites were chosen for  
225 near-natural flow characteristics. Examination of the study reaches in a GIS showed that most of  
226 the reaches were near small farm ponds ( $\leq 1$  km), some of the reaches were relatively near  
227 household water wells ( $\sim 200$ - $300$  m), and one reach contained a permitted surface water  
228 irrigation diversion, although it was unlikely to be active during the winter when the seepage run  
229 and temperature monitoring were conducted. None had instream impoundments.

#### 230 *Incremental Streamflow Method: Seepage Runs*

231 Seepage runs were performed at each site to validate the TEM (Figure 1, Table 2).  
232 Reaches were selected from candidate streams without flow contributions from tributary streams  
233 or major springs. Once identified, each reach was divided into three to five transects separated by  
234 200 to 500 m (Figure 1, Table 2). Discharge at each transect was measured with a RiverSurveyor  
235 M9 Acoustic Doppler Current Profiler (SonTek, San Diego, CA; hereafter ADCP). The  
236 enhanced density of transects per reach was established to achieve a smaller spatial scale which  
237 more closely matched the model setup used in the TEM while maintaining accurate groundwater  
238 flux estimation in consideration of instrument accuracy (error  $\leq \pm 0.015$  m<sup>3</sup>/s). At each reach, the  
239 ADCP-measured discharge at each transect was normalized for any flow changes detected at  
240 nearby USGS gauges during the sampling period to remove any temporal variation.

241 The normalized transect discharges were then regressed against the separation distance  
242 (upstream to downstream) with the slope of the regression representing the flux between the

243 stream and groundwater for the specific reach (Rosenberry and LaBaugh, 2008). Each seepage  
244 run included a flow and transect measurement at each logger site that were used to describe the  
245 channel geometry and hydrology in the model. The groundwater flux measurements were  
246 normalized by the streambed area (i.e., stream length and average ADCP transect width). Using  
247  $T_S$  measured instantaneously by the ADCP, the  $T_S$  difference among transects within each  
248 seepage run was determined to be less than 2°C, with this temperature variation likely due to  
249 diurnal temperature variations.

#### 250 *Stream Temperature and Atmospheric Time Series*

251 Temperature loggers (HOBO Water Temp Pro v2) were placed in the thalweg at each of  
252 the selected reaches. Hourly averaged  $T_S$  readings were recorded over a 15-d period in  
253 September 2016 on the Kiamichi River and June and December 2016 in the Ozark streams.  
254 Those times covered an extended low-flow period without any significant precipitation event. In  
255 the shallow Ozark streams, the loggers were placed at a depth between 0.3 and 1 m, and 1.0 to  
256 1.5 m in the deeper Kiamichi River.

257 A time series of air temperature, wind speed, solar radiation, and relative humidity was  
258 obtained for each site from the nearest Oklahoma Mesonet site (OCS, 2016), with the largest  
259 distance from a stream site being approximately 35 km for the Kiamichi River and  
260 approximately 40 km for the Ozark streams. The Mesonet stations are automated and collect data  
261 at 5-min increments, and reported an hourly average corresponding to the  $T_S$  time series. Note  
262 that there was some regional variation from site to site (Table 3), but the variation was not  
263 substantial. For the TEM approach, if users have meteorological data closer to their sites, they  
264 can easily use that data. In other words, the TEM approach should utilize the best available  
265 meteorological and hydrological data.

266

267 *Statistical Evaluation*

268 To validate the TEM, the FITEVAL software was used to evaluate the fit between  
269 groundwater fluxes measured from seepage runs and predicted by the TEM. FITEVAL is a  
270 software tool that uses procedures presented by Ritter and Muñoz-Carpena (2013) to incorporate  
271 both data and model uncertainty into standardized model evaluation. FITEVAL conducts model  
272 evaluations using a combination of graphical illustrations, absolute value error statistics (root  
273 mean square error, RMSE), and normalized goodness-of-fit statistics (Nash–Sutcliffe Efficiency  
274 coefficient, NSE). Bias corrected confidence intervals are calculated based on approximated  
275 probability distributions derived from bootstrapping, followed by hypothesis test results of the  
276 indicators, helping to reduce subjectivity in the interpretation of the model performance (Ritter  
277 and Muñoz-Carpena, 2013).

278 **Results and Discussion**279 *TEM versus Seepage Runs*

280 Model validation suggested that TEM was a suitable technique for estimating  
281 groundwater flux into streams. The groundwater flux into the streams measured via seepage runs  
282 ranged from 0.01 to 1.09 m/d and from 0.00 to 0.95 m/d with the TEM (Table 4). The estimated  
283 groundwater flux at the Ozark sites was generally higher than at the Kiamichi sites as expected.  
284 The resulting RMSE and NSE for the TEM fit to the seepage run data from FITEVAL were 0.08  
285 (m/d) and 0.93, respectively, indicated a very good fit. Linear regression analysis showed a  
286 uniform variance across the range of estimates with an  $R^2$  of 0.94 (Figure 5). However, the TEM  
287 tended to under predict the seepage run flux estimates by -5.7% (Figure 5). An example

288 continuous application of the TEM at a weekly time scale is shown in Figure 6 for one of the  
289 sites. The corresponding groundwater flux estimated by the seepage run is also shown in the  
290 figure.

291 Deviations are to be expected between the two measurements. The seepage run represents  
292 a spatially integrated flux estimate over a small temporal scale (~2 hr), whereas the TEM  
293 represented a temporally integrated flux estimate of a small spatial scale. More specifically,  
294 during a seepage run, locally alternating gaining and losing sections of the stream are integrated  
295 into this spatially integrated measurement. These two estimates were similar suggesting that the  
296 groundwater flux into these streams may not vary widely over the approximately 1.5 km of  
297 stream length or the 15-d time period used in this study. Also, the seepage runs measured the net  
298 groundwater exchange. If the groundwater discharge along a reach was exactly balanced with the  
299 groundwater recharge, then the net change of streamflow would not be detected. The TEM  
300 method, however, will quantify the groundwater inflow because it generates a temperature signal.  
301 This difference may explain situations when the TEM method overestimated the groundwater  
302 flux compared to that measured during the seepage runs, e.g. Kiamichi River. Future research  
303 should examine the prediction from TEM further by comparison against estimates derived from  
304 other methods at different times of the year and with temporal scales that align better with TEM.

305 Other than the groundwater flux, the expanded domain length was the only model  
306 parameter not represented by measurements; therefore, it was important to examine that  
307 parameter and its influence on the groundwater flux results. The model domain in the TEM was  
308 a 2-km conceptual stream reach composed of twenty segments of 100 m each. To test the effect  
309 of model domain length, groundwater flux for Spavinaw Creek in northwest Arkansas was  
310 estimated with TEM using alternate total domain lengths of 0.2 and 20 km, each with twenty

311 equal length segments. The estimated groundwater fluxes (indicated by the minimum of SSE  
312 between the upstream and downstream boundaries) were identical for the 0.2- and 2-km domains,  
313 but larger for the 20-km domain. This is likely due to the accumulation of groundwater flux over  
314 an extensive simulation distance that significantly changed the heat capacity of the stream. For  
315 example, at Spavinaw Creek the average flow rate was  $2 \text{ m}^3/\text{s}$ , and the total estimated  
316 groundwater flux accumulation over a 2-km model domain was  $0.1 \text{ m}^3/\text{s}$ ; a difference that is  
317 unlikely to significantly change the energy balance of the stream. In contrast, the total  
318 groundwater flux accumulation over a 20-km model domain was  $1.0 \text{ m}^3/\text{s}$  with the same rate of  
319 groundwater flux, an increase that greatly affected the stream heat capacity.

320 Since the design of the model domain also affects runtime, some test runs with different  
321 domain dimensions may be helpful to balance accuracy and processing time. The temperature  
322 module of WASP applied the given thermal and stream parameters sequentially to each segment  
323 using a variable internal time-step to reach satisfactory convergence. For the test simulations  
324 mentioned above, the run time of the 0.2-km model domain extended to over an hour, whereas  
325 the 2-km domain took only 7 to 10 minutes. This was likely due to the extra iterations required  
326 for time-dependent thermal processes to converge in the reduced length of the smaller domain.

327 *Where is TEM applicable?*

328 Due to the one-dimensional nature of the temperature model used in TEM, the method  
329 was most appropriate for shallow, well-mixed streams that were unlikely to exhibit stratified  
330 zones of temperature or flow. A groundwater temperature signature, defined as the temperature  
331 difference between  $T_{AE}$  and  $T_E$  caused by groundwater flux, was required for the TEM to predict  
332 effectively. Streams with low flow and no groundwater flux tend to equilibrate at a high  
333 temperature during warm weather conditions ( $T_E = T_{AE}$ ). In contrast, streams with groundwater

334 flux cooler than stream water equilibrate at a lower temperature during warm weather conditions  
335 ( $T_E < T_{AE}$ ), causing a temperature signature that could be used to quantify groundwater flux  
336 through TEM. However, groundwater recharge (i.e., losing streams) would not result in a similar  
337 temperature signature, and thus could not be quantified by the TEM. Similarly, when  $T_S$   
338 approximate groundwater temperatures during certain times of the year (Figure 3) (Briggs et al.,  
339 2016; Kurylyk et al., 2016), the temperature signature of the groundwater flux would be difficult  
340 to detect. Therefore, the TEM is most effective where the temperature signature of groundwater  
341 flux is strong, i.e., gaining reaches and seasons when groundwater temperatures deviate from  $T_S$ .  
342 Nevertheless, the change in heat capacity caused by the loss or addition of stream water volume  
343 will lead to an altered  $T_S$  temporal variance. Future research with higher data precision may be  
344 able to identify the altered  $T_S$  variance and use it to quantify groundwater interactions similarly  
345 to TEM.

346 To improve the robustness of the thermal equilibrium assumption, it is important to  
347 consider the location of the  $T_S$  monitoring point and the sampling duration. When groundwater  
348 flux changes gradually, stream water remains at thermal equilibrium and therefore  $T_S = T_E$   
349 (Figure 7). In contrast, upwelling zones, where there would be an abrupt change in groundwater  
350 flux, would cause a loss of thermal equilibrium that recovers over some downstream distance ( $T_S$   
351  $\neq T_E$ ). Groundwater flux estimates made at any point at thermal equilibrium represented the true  
352 magnitude of groundwater flux into the stream at that point. Estimates made at points where  
353 thermal equilibrium is recovering would yield an inaccurate groundwater flux because the  $T_S$   
354 does not meet the primary assumption of the TEM. Although an investigator is unlikely to have  
355 prior knowledge of the spatial distribution of groundwater interactions in a particular stream, it  
356 would be advantageous to avoid placing temperature loggers at locations with drastically varying

357 temperatures. Moreover, based on previous research, we suggest that at least one week of  $T_S$  time  
358 series should be collected for the thermal equilibrium assumption to be met (Bogan et al., 2003).

### 359 **Conclusions**

360 The TEM proposed in this research has several advantages to researchers interested in  
361 characterizing stream and groundwater interactions as long as the primary assumptions of the  
362 approach are met. With this approach, only  $T_S$  is needed at a single point to monitor groundwater  
363 flux. This can also potentially add significant value to  $T_S$  data typically collected in stream  
364 biology studies (Hawkins et al., 1997), and  $T_S$  data are readily available at a number of USGS  
365 gage locations. Although a minimum of one week of  $T_S$  data is recommended to satisfy the  
366 thermal equilibrium assumption (Bogan et al., 2003), the TEM can be used to estimate  
367 groundwater flux at any temporal scale coarser than one week (i.e., monthly, seasonally or  
368 yearly). Similarly, the proposed method has the potential to economically quantify spatial  
369 differences in groundwater fluxes at multiple stream points or to create a flux estimate for a large  
370 area if applied in an array. The main limitation of the TEM is that it requires a detectable and  
371 equilibrated temperature signature of groundwater flux. Another weakness of the method, and  
372 one that it shares with other model approaches, is that the precision of groundwater flux is  
373 heavily dependent on the availability and quality of the input data. Our study utilized  
374 atmospheric and solar radiation data from the Oklahoma Mesonet; however similar systems exist  
375 or are being installed in other many other states. Finally, the approach performs best in well-  
376 mixed shallow streams because those conditions most closely match the one-dimensional model  
377 structure.

378 **Acknowledgements**

379 This research is a contribution of the North Carolina Agricultural Research Service and the  
380 Oklahoma Cooperative Fish and Wildlife Research Unit (U.S. Geological Survey, Oklahoma  
381 Department of Wildlife Conservation, Oklahoma State University, and Wildlife Management  
382 Institute cooperating). The National Science Foundation (Grant No. OIA-1301789) and the  
383 Oklahoma Department of Wildlife Conservation (Grant No. F13AF01327) provided project  
384 funding. We thank Justin Alexander for technical assistance. The author Y Zhou was supported  
385 in part by a scholarship from the China Scholarship Council (CSC) (Grant CSC No.  
386 201306306300023). Any use of trade, firm, or product names is for descriptive purposes only  
387 and does not imply endorsement by the U.S. Government. The authors acknowledge Dr. Daniel  
388 Storm and Dr. Chris Zou, Oklahoma State University, and Dr. Derek Heeren, University of  
389 Nebraska-Lincoln, for reviewing an earlier version of this manuscript.

390 **References**

- 391 Adamski, J. C., Petersen, J. C., Freiwald, D. A., Davis, J. V., 1995. Environmental and  
392 hydrologic setting of the Ozark Plateaus study unit, Arkansas, Kansas, Missouri, and  
393 Oklahoma. *US Geological Survey Water-Resources Investigations Report*, **94-4022**,  
394 Little Rock, AR.
- 395 Allison, G., Hughes, M., 1975. The use of environmental tritium to estimate recharge to a South-  
396 Australian aquifer. *Journal of Hydrology*, **26**(3): 245-254.
- 397 Anderson, M. P., 2005. Heat as a ground water tracer. *Groundwater*, **43**(6): 951-968.
- 398 Arnold, J., Allen, P., Muttiah, R., Bernhardt, G., 1995. Automated base flow separation and  
399 recession analysis techniques. *Groundwater*, **33**(6): 1010-1018.

- 400 Barlocher, F., Murdoch, J. H., 1989. Hyporheic biofilms—a potential food source for interstitial  
401 animals. *Hydrobiologia*, **184**(1-2): 61-67.
- 402 Becker, M., Georgian, T., Ambrose, H., Siniscalchi, J., Fredrick, K., 2004. Estimating flow and  
403 flux of ground water discharge using water temperature and velocity. *Journal of*  
404 *Hydrology*, **296**(1): 221-233.
- 405 Berry, L., Mutiti, S., Hazzard, S., 2011. Determining the Hydraulic Conductivity of the  
406 Subsurface in Wetland Environments, AGU Fall Meeting Abstracts.
- 407 Blasch, K. W., Constantz, J., Stonestrom, D. A., 2007. Thermal methods for investigating  
408 ground-water recharge. in Stonestrom, D. A., Constantz, J., Ferre, T., and Leake, S. A.,  
409 eds., Ground-water recharge in the arid and semiarid southwestern United States, U.S.  
410 Geological Survey Professional Paper 1703, Appendix 1, p. 351-373.
- 411 Bogan, T., Mohseni, O., Stefan, H. G., 2003. Stream temperature-equilibrium temperature  
412 relationship. *Water Resources Research*, **39**(9), doi: 10.1029/2003WR002034.
- 413 Bogan, T., Stefan, H. G., Mohseni, O., 2004. Imprints of secondary heat sources on the stream  
414 temperature/equilibrium temperature relationship. *Water Resources Research*, **40**(12), doi:  
415 10.1029/2003WR002733.
- 416 Bredehoeft, J., Papaopulos, I., 1965. Rates of vertical groundwater movement estimated from the  
417 Earth's thermal profile. *Water Resources Research*, **1**(2): 325-328.
- 418 Briggs, M., Johnson, Z. C., Snyder, C., Hitt, N. P., White, E. A., Lane, J. W., Jr., Nelms, D. L.,  
419 2016. Strong seepage of shallow groundwater shifts the timing of the annual thermal  
420 signals in stream water, American Geophysical Union, Fall General Assembly 2016,  
421 abstract #H32E-05.

- 422 Brock, F. V., Crawford, K. C., Elliott, R. L., Cuperus, G. W., Stadler, S. J., Johnson, H. L., Eilts,  
423 M. D., 1995. The Oklahoma Mesonet: A technical overview. *Journal of Atmospheric and*  
424 *Oceanic Technology*, **12**: 5-19.
- 425 Brodie, R., Sundaram, B., Tottenham, R., Hostetler, S., Ransley, T., 2007. An overview of tools  
426 for assessing groundwater-surface water connectivity. Bureau of Rural Sciences,  
427 Canberra.
- 428 Cole, T., Buchak, E., 1995. A two-dimensional, laterally averaged, hydrodynamic and water  
429 quality model, Version 2.0 User Manual. Instruction Report EL-95. US Army Corps of  
430 Engineers, Waterways Experiment Station, Vicksburg, MS.
- 431 Constantz, J., 1998. Interaction between stream temperature, streamflow, and groundwater  
432 exchanges in alpine streams. *Water Resources Research*, **34**(7): 1609-1615.
- 433 Constantz, J., 2008. Heat as a tracer to determine streambed water exchanges. *Water Resources*  
434 *Research*, **44**(4), doi: 10.1029/2008WR006996.
- 435 Cook, P., Solomon, D. K., 1997. Recent advances in dating young groundwater:  
436 chlorofluorocarbons,  $^3\text{H}^3\text{He}$  and  $^{85}\text{Kr}$ . *Journal of Hydrology*, **191**(1): 245-265.
- 437 Donato, M. M. 1998. Surface-water/ground-water relations in the Lemhi River Basin, East-  
438 Central Idaho. Water Resources Investigations Report 98-4185, U.S. Geological Survey,  
439 Denver, CO.
- 440 Eriksson, E., Khunakasem, V., 1969. Chloride concentration in groundwater, recharge rate and  
441 rate of deposition of chloride in the Israel Coastal Plain. *Journal of Hydrology*, **7**(2): 178-  
442 197.
- 443 Freeze, R., Cherry, J., 1979. Groundwater. Prentice Hall: Englewood Cliffs, NJ.

- 444 Harvey, J. W., Wagner, B. J., 2000. Quantifying hydrologic interactions between streams and  
445 their subsurface hyporheic zones. In *Streams and Ground Waters*, Jones, J.B.,  
446 Mulholland, P. J. (eds.), Academic Press, San Diego, CA.
- 447 Hawkins, C. P., Hogue, J. N., Decker, L. M., Feminella, J. W., 1997. Channel morphology, water  
448 temperature, and assemblage structure of stream insects. *Journal of the North American*  
449 *Benthological Society*, **16**(4): 728-749.
- 450 Kalbus, E., Reinstorf, F., Schirmer, M., 2006. Measuring methods for groundwater, surface  
451 water and their interactions: a review. *Hydrology and Earth System Sciences Discussions*,  
452 **3**(4): 1809-1850.
- 453 Kurylyk, B. L., Bourque, C.-A., MacQuarrie, K., 2013. Potential surface temperature and  
454 shallow groundwater temperature response to climate change: an example from a small  
455 forested catchment in east-central New Brunswick (Canada). *Hydrology and Earth*  
456 *System Sciences*, **17**(7): 2701-2716.
- 457 Kurylyk, B. L., Moore, R. D., MacQuarrie, K. T., 2016. Scientific briefing: quantifying  
458 streambed heat advection associated with groundwater–surface water interactions.  
459 *Hydrological Processes*, **30**(6): 987-992.
- 460 Lapham, W. W., 1989. Use of temperature profiles beneath streams to determine rates of vertical  
461 ground-water flow and vertical hydraulic conductivity. U.S. Geological Survey Water-  
462 Supply Paper 2337, U.S. Geological Survey: Denver, CO.
- 463 Laursen, A., Seitzinger, S., 2005. Limitations to measuring riverine denitrification at the whole  
464 reach scale: effects of channel geometry, wind velocity, sampling interval, and  
465 temperature inputs of N<sub>2</sub>-enriched groundwater. *Hydrobiologia*, **545**(1): 225-236.

- 466 Lee, D. R., 1985. Method for locating sediment anomalies in lakebeds that can be caused by  
467 groundwater flow. *Journal of Hydrology*, **79**(1): 187-193.
- 468 Loinaz, M. C., Davidsen, H. K., Butts, M., Bauer-Gottwein, P., 2013. Integrated flow and  
469 temperature modeling at the catchment scale. *Journal of Hydrology*, **495**: 238-251.
- 470 Loheide, S. P., Gorelick, S. M., 2006. Quantifying stream– aquifer interactions through the  
471 analysis of remotely sensed thermographic profiles and in situ temperature histories.  
472 *Environmental Science & Technology*, **40**(10): 3336-3341.
- 473 Malard, F., Hervant, F., 1999. Oxygen supply and the adaptations of animals in groundwater.  
474 *Freshwater Biology*, **41**(1): 1-30.
- 475 Miller, J. A., Appel, C., 1997. Ground water atlas of the United States: Kansas, Missouri and  
476 Nebraska. HA 730-D. US Geological Survey: Denver, CO.
- 477 Nigh, T. A., Schroeder, W. A., 2002. Atlas of Missouri ecoregions. Missouri Department of  
478 Conservation: Jefferson City, MO.
- 479 Pluhowski, E. J., 1970. Urbanization and its effect on the temperature of the streams on Long  
480 Island, New York. Professional Paper 627-D, U.S. Geological Survey: Washington, D.C.
- 481 Pyron, M., Vaughn, C. C., Winston, M. R., Pigg, J., 1998. Fish assemblage structure from 20  
482 years of collections in the Kiamichi River, Oklahoma. *The Southwestern Naturalist*, **43**(3):  
483 336-343.
- 484 Ritter, A., Muñoz-Carpena, R., 2013. Performance evaluation of hydrological models: Statistical  
485 significance for reducing subjectivity in goodness-of-fit assessments. *Journal of*  
486 *Hydrology*, **480**: 33-45.

- 487 Rosenberry, D. O., LaBaugh, J. W., 2008. Field techniques for estimating water fluxes between  
488 surface water and ground water. U.S. Geological Survey Techniques and Methods 4-D2,  
489 U.S. Geological Survey: Reston, VA.
- 490 Rutledge, A., 1998. Computer programs for describing the recession of ground-water discharge  
491 and for estimating mean ground-water recharge and discharge from streamflow records:  
492 Update. U.S. Geological Survey, Water-Resources Investigations Report 98-4148, U.S.  
493 Geological Survey: Reston, VA.
- 494 Scanlon, B. R., Healy, R. W., Cook, P. G., 2002. Choosing appropriate techniques for  
495 quantifying groundwater recharge. *Hydrogeology Journal*, **10**(1): 18-39.
- 496 Schmidt, C., Conant, B., Bayer-Raich, M., Schirmer, M., 2007. Evaluation and field-scale  
497 application of an analytical method to quantify groundwater discharge using mapped  
498 streambed temperatures. *Journal of Hydrology*, **347**(3): 292-307.
- 499 Silliman, S. E., Booth, D. F., 1993. Analysis of time-series measurements of sediment  
500 temperature for identification of gaining vs. losing portions of Juday Creek, Indiana.  
501 *Journal of Hydrology*, **146**: 131-148.
- 502 Sinokrot, B. A., Stefan, H. G., 1993. Stream temperature dynamics: Measurements and modeling.  
503 *Water Resources Research*, **29**(7): 2299-2312.
- 504 Smith, K., 1981. The prediction of river water temperatures. *Hydrological Sciences Journal*,  
505 **26**(1): 19-32.
- 506 Sophocleous, M., Perkins, S. P., 2000. Methodology and application of combined watershed and  
507 ground-water models in Kansas. *Journal of Hydrology*, **236**(3): 185-201.

- 508 Stallman, R., 1965. Steady one-dimensional fluid flow in a semi-infinite porous medium with  
509 sinusoidal surface temperature. *Journal of Geophysical Research*, **70**(12): 2821-2827.
- 510 Stofleth, J. M., Shields Jr, F. D., Fox, G. A., 2008. Hyporheic and total transient storage in small,  
511 sand-bed streams. *Hydrological Processes*, **22**(12): 1885-1894.
- 512 Suzuki, S., 1960. Percolation measurements based on heat flow through soil with special  
513 reference to paddy fields. *Journal of Geophysical Research*, **65**(9): 2883-2885.
- 514 Taniguchi, M., Fukuo, Y., 1993. Continuous measurements of ground-water seepage using an  
515 automatic seepage meter. *Groundwater*, **31**(4): 675-679.
- 516 Turner, J. V., 2009. Estimation and prediction of the exchange of groundwater and surface water:  
517 field methodologies. eWater Technical Report, eWater Cooperative Research Centre,  
518 Canberra.
- 519 USGS. 2017. Comparison of selected methods for estimating groundwater recharge in humid  
520 regions. <https://water.usgs.gov/ogw/gwrp/methods/compare/>, Accessed 16 Oct. 2017.
- 521 Webb, B. W., Hannah, D. M., Moore, R. D., Brown, L. E., Nobilis, F., 2008. Recent advances in  
522 stream and river temperature research. *Hydrological Processes*, **22**(7): 902-918.
- 523 Westhoff, M., Savenije, H., Luxemburg, W., Stelling, G., van de Giesen, N., Selker, J., Pfister,  
524 L., Uhlenbrook, S., 2007. A distributed stream temperature model using high resolution  
525 temperature observations. *Hydrology and Earth System Sciences*, **11**(4): 1469-1480. doi:  
526 10.5194/hess-11-1469-2007.
- 527 Wool, T. A., Ambrose, R. B., Martin, J. L., Comer, E. A., 2006. Water Quality Analysis  
528 Simulation Program (WASP) User's Manual, Version 6. U.S. Environmental Protection  
529 Agency: Atlanta, GA.

- 530 Zamora, C., 2008. Estimating water fluxes across the sediment-water interface in the lower  
531 Merced River, California. U.S. Geological Survey Scientific Investigations Report 2007-  
532 5216, U.S. Geological Survey: Reston, VA.
- 533 Zhou, Y., Wilson, G., Fox, G. A., Rigby, J., Dabney, S., 2016. Soil pipe flow tracer experiments:  
534 2. Application of a streamflow transient storage zone model. *Hydrological Processes*,  
535 **30**(8): 1280-1291.
- 536

**Table 1. Comparison of common methods for estimating groundwater discharge to/from streams (adapted from USGS, 2017).**

Category	Method	Spatial Scale	Temporal Scale	Typical Quantity Estimated	Ease of Use	Data Needs	Relative Cost	Reference
Water Budget	Groundwater Modeling	Local / Regional	Month to Years	Recharge	Moderate	High	High	Sophocleous and Perkins (2000)
	Watershed Models	Watershed /Regional	Days to Years	Recharge	Moderate	High	High	Sophocleous and Perkins (2000)
Darcian	Piezometers	Point	Instantaneous	Potential Recharge	Moderate	Low	High	Stofleth et al. (2008)
Streamflow	Seepage Meters	Point	Event to Months	Potential Recharge	Moderate	Low	Low	Taniguchi and Fukuo (1993)
	Stream Base-Flow Analysis	Watershed	Years	Net Recharge	Easy	Low	Low	Arnold et al. (1995)
	Incremental Streamflow Method (Seepage Run)	Local	Instantaneous	Potential Recharge	Easy	Low	Low	Rosenberry and LaBaugh (2008)
	Recession-Curve Displacement Method	Watershed	Event to Years	Net Recharge	Moderate	Low	Low	Rutledge (1998)
Tracer	Chloride	Point	Years	Recharge	Easy	Moderate	Moderate	Eriksson and Khunakasem (1969)
	Chlorofluorocarbons	Local	Month to Years	Recharge	Difficult	Moderate	High	Cook and Solomon (1997)
	Temperature	Point	Days to Years	Recharge	Moderate	Moderate	High	Constantz (2008)
	Tritium	Point	Month to Years	Recharge	Moderate	Moderate	High	Allison and Hughes (1975)

**Table 2. Characteristics of the seepage runs performed to quantify groundwater flux into streams.**

Site Name	Upstream Boundary		Downstream Boundary		Date Performed	Measurement Period	Number of Transects
	Latitude	Longitude	Latitude	Longitude	Year/Month/Day	(hr)	
NDN	34.6597	-95.0307	34.6578	-95.0415	2016/7/6	2.4	4
Robins	34.6361	-95.125	34.6270	-95.1267	2016/7/7	1.8	4
JFC up	34.5986	-95.3281	34.5976	-95.336	2016/7/7	1.4	4
JFC down	34.5959	-95.3368	34.5895	-95.3395	2016/7/7	1.2	3
Payne	34.4255	-95.5765	34.4190	-95.5727	2016/7/8	1.8	3
Spavinaw	36.3245	-94.7063	36.3214	-94.7142	2017/1/11	1.1	3
Honey	36.5401	-94.7036	36.5428	-94.7111	2017/1/10	1.3	3
Caney	35.7927	-94.8475	35.7886	-94.8499	2016/6/7	2.2	4
Buffalo	36.6396	-94.6273	36.6356	-94.6303	2017/1/11	1.3	3
Saline	36.2896	-95.0847	36.2850	-95.0917	2017/1/11	1.0	3
Caney 2	35.7927	-94.8475	35.7886	-94.8499	2017/1/12	1.6	4
Greenleaf	35.7523	-95.0472	35.7410	-95.0591	2017/1/13	2.0	5
Spavinaw 2	36.3495	-94.5666	36.3335	-94.6386	2017/6/22	2.3	4
Spavinaw 3	36.3297	-94.6468	36.3271	-94.6685	2017/6/22	2.2	3

**Table 3. Regional variations of air temperature (°C), dew point temperature (°C), wind speed (m/s), and solar radiation (W/m<sup>2</sup>) monitored at Mesonet stations located near the Kiamichi River in September 2016 and in the Ozark Highland Ecoregion in June and December 2016, showing their averages, errors and p-value of paired t-tests. Atmospheric conditions monitored at Clayton Station were compared to those at two nearby Mesonet Stations: Talihina (36 km away) and Antlers (67 km away). Atmospheric conditions monitored at Jay were compared to those at the nearby Mesonet station at Westville (67 km away).**

		Air Temperature (°C)	Dew Point (°C)	Wind Speed (m/s)	Solar Radiation (W/m <sup>2</sup> )
<i>Kiamichi River – September 2016</i>					
Clayton	Average	23.63	18.58	1.56	232.43
	Average	23.45	18.45	1.83	233.16
Talihina	Error	-0.18	-0.13	0.27	0.73
	p-Value	0.00	0.00	0.00	0.74
Antlers	Average	23.57	18.99	1.55	226.03
	Error	-0.05	0.41	-0.01	-6.41
	p-Value	0.26	0.00	0.76	0.01
<i>Ozark Highland Ecoregion – June 2016</i>					
Jay	Average	25.16	20.31	1.77	305.34
	Average	25.28	19.83	1.91	301.08
Westville	Error	0.12	-0.48	0.14	-4.26
	p-Value	0.00	0.00	0.00	0.07
<i>Ozark Highland Ecoregion – December 2016</i>					
Jay	Average	4.58	-1.90	3.02	84.93
	Average	5.33	-0.85	3.36	81.76
Westville	Error	0.75	1.05	0.34	-3.18
	p-Value	0.00	0.00	0.00	0.43

**Table 4. Comparison of groundwater flux (m/d) estimated by seepage run and thermal equilibrium methods for each sample site. Stream water and air temperature (°C) during the simulation period were averaged and reported as  $T_w$  and  $T_a$  respectively.**

Watershed	Site Name	Groundwater Flux Estimate			Stream Temperature, $T_w$ (°C)	Air Temperature, $T_a$ (°C)
		Seepage Run, SR (m/d)	Thermal Equilibrium Method, TEM (m/d)	Relative Difference*		
Kiamichi River	NDN	0.11	0.08	-27	24.5	19.2
	Robins	0.14	0.10	-29	22.2	19.2
	JFC up	0.08	0.11	38	22.4	19.2
	JFC down	0.01	0.12	1100**	22.4	19.2
	Payne	0.01	0.08	700	22.8	19.2
Ozark Highland Ecoregion	Spavinaw	0.38	0.46	21	9.8	3.3
	Honey	0.74	0.65	-12	10.4	8.1
	Caney	0.35	0.32	-9	9.3	5.7
	Buffalo	0.61	0.63	3	10.7	2.9
	Saline	0.66	0.54	-18	10.6	2.9
	Caney 2	0.15	0.05	-67	9.5	3.4
	Greenleaf	0.09	0.00	-100	7.1	3.4
	Spavinaw 2	0.56	0.61	9	21.0	24.4
Spavinaw 3	1.09	0.95	-13	21.2	24.4	

\* Calculated as (TEM-SR)/SR x 100%

\*\* Large relative percent differences were due to low groundwater fluxes measured during the seepage run

## Figure Captions

Figure 1. Diagram of the application of the thermal equilibrium method (TEM) and seepage run segment at one of the sites. Diamonds in the seepage run segment represent measurement transects. The TEM assumes stream water temperatures are at thermal equilibrium with the combination of atmospheric conditions and groundwater interactions at the monitoring point. The monitoring point was expanded to a hypothetical model domain to investigate the thermal equilibrium reached at the monitoring point and consequently solve for the unknown groundwater flux.

Figure 2. Temperature module of the thermal equilibrium method showing (a) the twenty segment model domain, (b) upstream boundary conditions derived from stream water temperature ( $T_S$ ) and flow monitoring, (c) atmospheric heat transfer parameters applied to each model segment at each time step, and (d) the predicted equilibrium water temperature ( $T_E$ ). The magnitude of the groundwater flux (e) at a given temperature is calibrated to minimize the sum of squared errors between the measured stream temperature and predicted equilibrium temperature at the downstream boundary. Most variables are defined in equations (1) and (2). Note that  $\beta$  is the fraction of short wave radiation adsorbed at the water surface,  $z$  is depth,  $C_c$  is Bowen's coefficient,  $\varepsilon$  is the emissivity of water (0.97), and  $\sigma$  is the Stephan-Boltzman constant.

Figure 3. Daily averaged stream water temperatures time series compared to groundwater for 2015. Stream water temperature time series were monitored on Big Cedar USGS gauge, and groundwater temperature was estimated using air temperature retrieved from Talihina Mesonet Station 15 miles away with 1.5-month time lag as recommended by Pluhowski (1970). Solid and dotted lines represent fitted sine curves for stream water and groundwater temperatures, respectively. The vertical lines indicate intersections of the fitted curves where there is no estimated difference between the measured stream water and the estimated groundwater temperatures, and the thermal equilibrium method cannot estimate groundwater flux.

Figure 4. Study sites on the Kiamichi River (bottom left) and Ozark Highland Ecoregion (top left). Oklahoma Mesonet stations and USGS gages are represented by triangle and diamond markers, respectively. Cross markers indicate monitoring sites where stream water temperature data were collected and seepage runs were performed.

Figure 5. FITEVAL evaluation and regression results comparing groundwater fluxes estimated by seepage run and thermal equilibrium method. Plots showing (a) regression of seepage run and thermal equilibrium method groundwater flux estimates, (b) FITEVAL plot of cumulative probability of Nash-Sutcliffe Efficiency (NSE), with the median value indicating the reported NSE, (c) FITEVAL model diagnostic report including hypothesis test results, outliers, and the

sensitivity of the indicators to model bias, and (d) scatter plot showing fit between seepage run and thermal equilibrium method groundwater flux estimates in order of the series. Actual values are shown in Table 2.

Figure 6. Example continuous application of the thermal equilibrium method (TEM) for Buffalo Creek for five weeks from 19 December 2016 to 22 January 2017. The TEM application shown was at a weekly time scale. The groundwater flux estimated from the seepage run performed on 11 January 2017 is also shown.

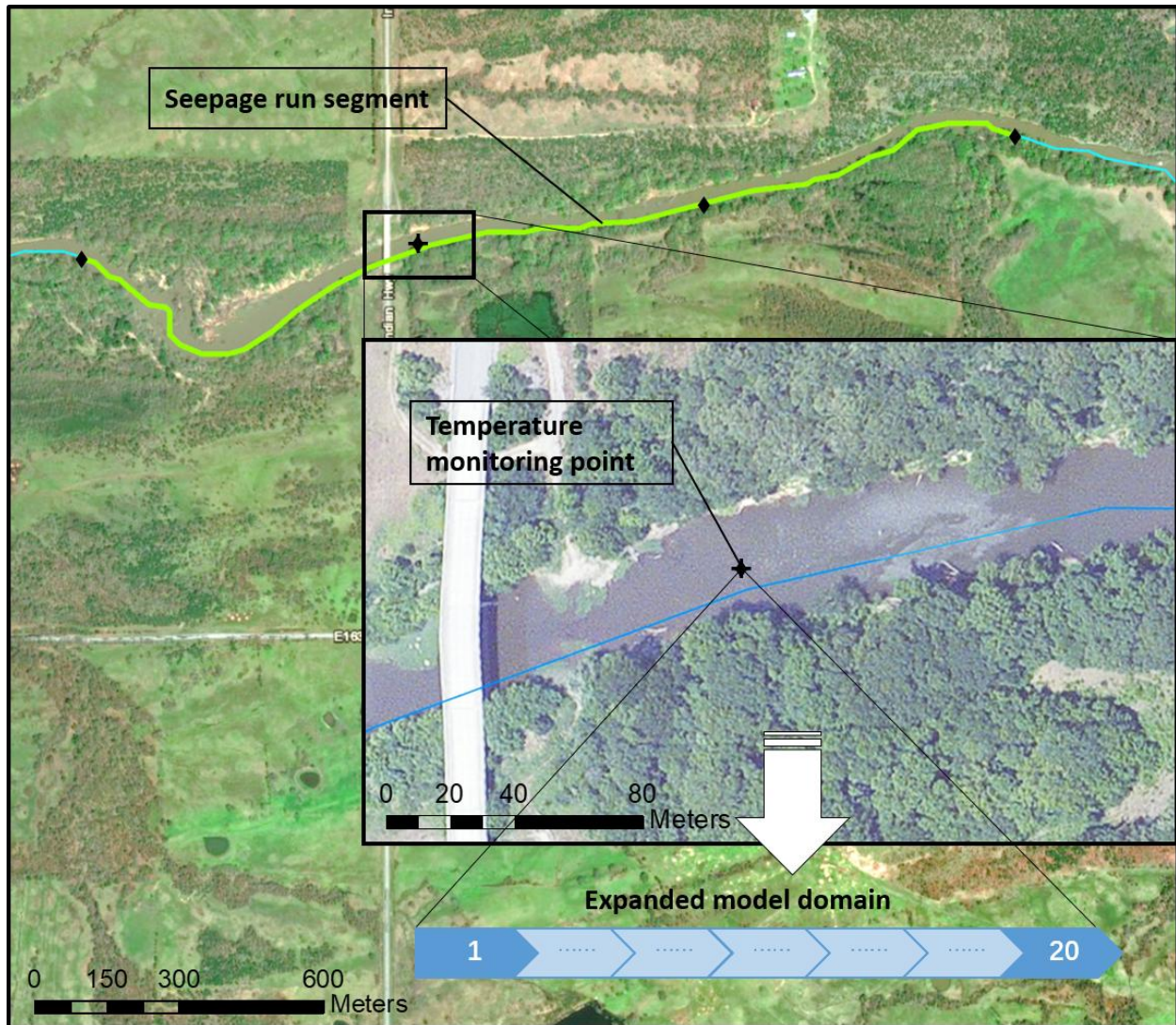
Figure 7. Temperature of a hypothetical stream in the presence of cooler groundwater flux. (a) Stream water temperatures ( $T_S$ ) remain at equilibrium at the presence of gradual changing groundwater flux, and (b) loss of thermal equilibrium due to changing groundwater flux. The thermal equilibrium method provides an accurate estimate of the groundwater flux for any point at thermal equilibrium. Estimates made with the thermal equilibrium method where  $T_S \neq T_E$  will not represent an accurate flux.

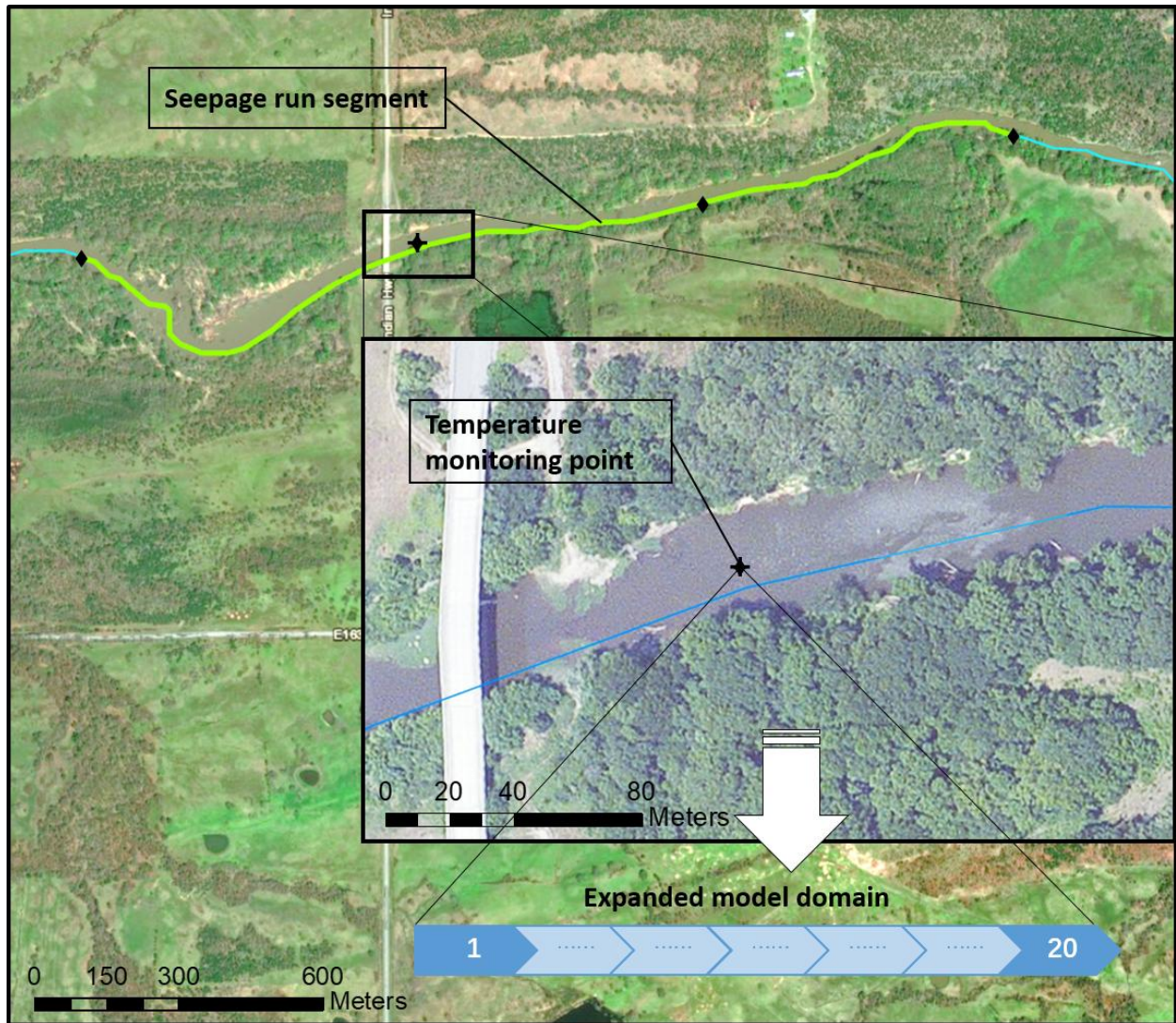
## Groundwater Flux Estimation in Streams: A Thermal Equilibrium Approach

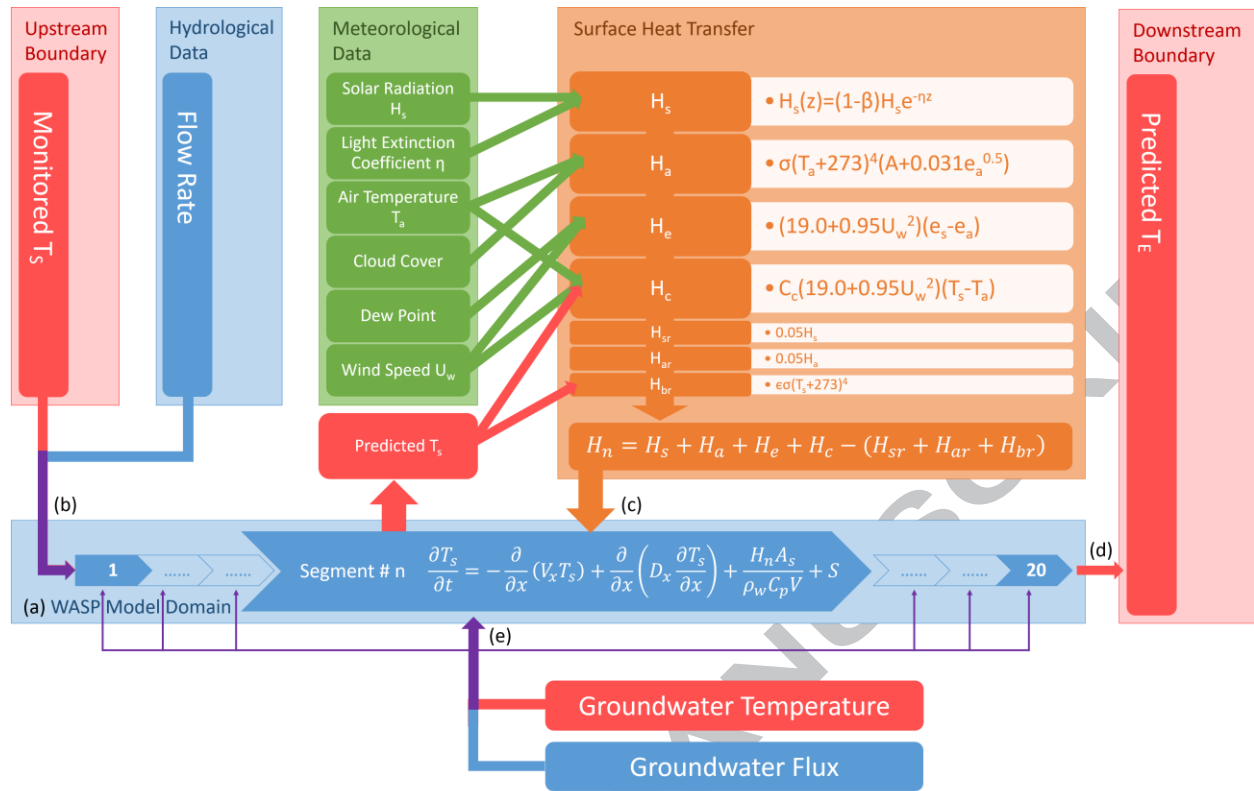
### Research Highlights

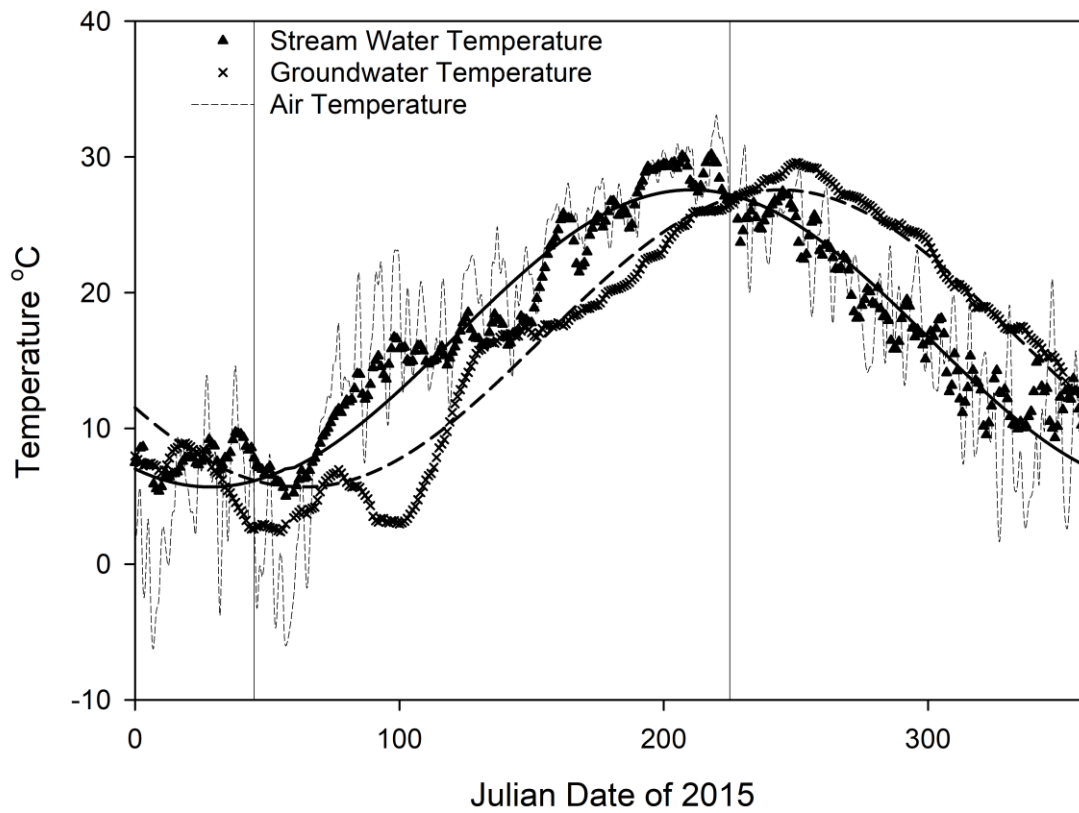
- ▶ A thermal equilibrium method was developed to quantify point groundwater flux.
- ▶ The primary assumption was thermal equilibrium at the temperature monitoring point.
- ▶ The predictions matched well statistically with measurements from seepage runs.
- ▶ The method requires a groundwater temperature signature to work effectively.

## Graphical abstract

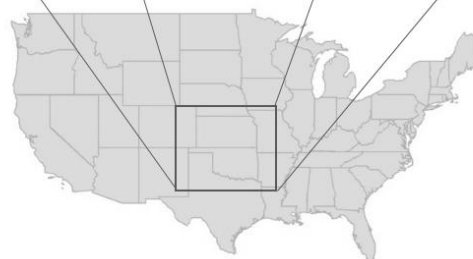
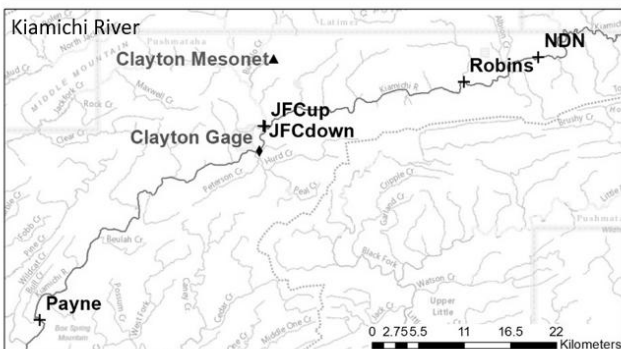
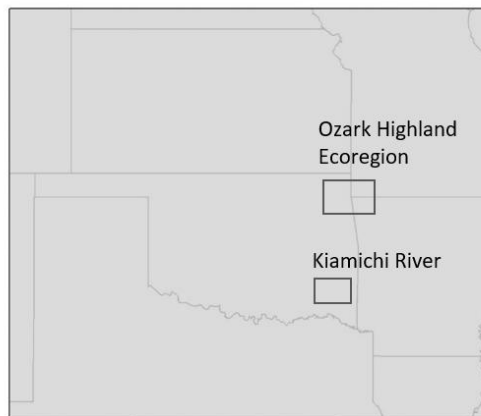
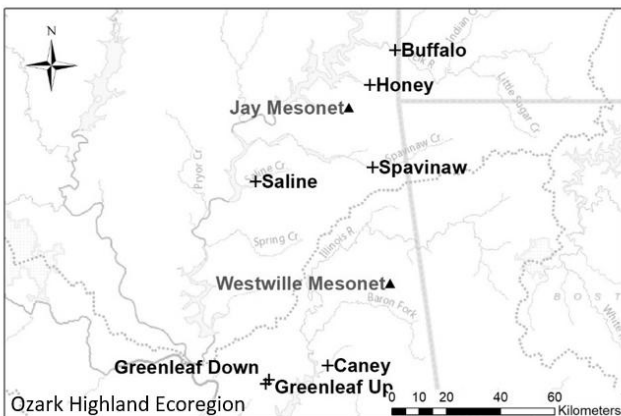




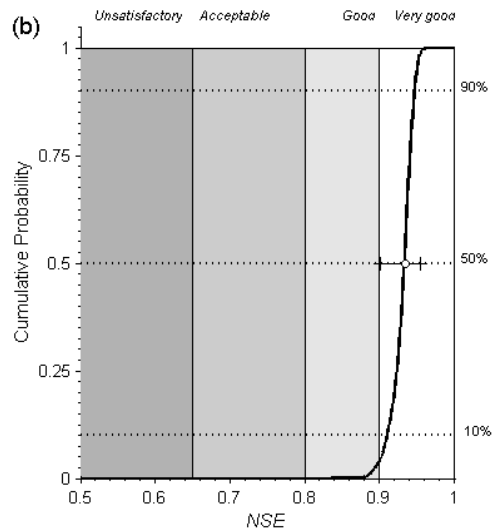
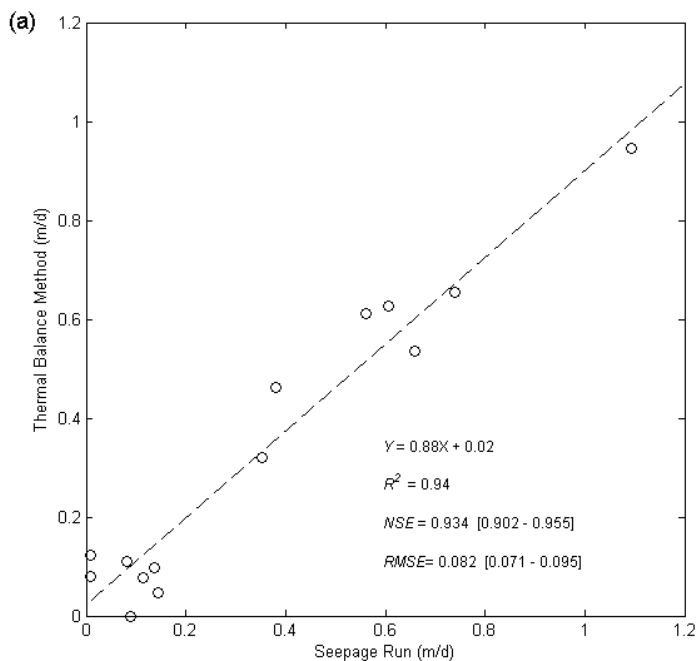




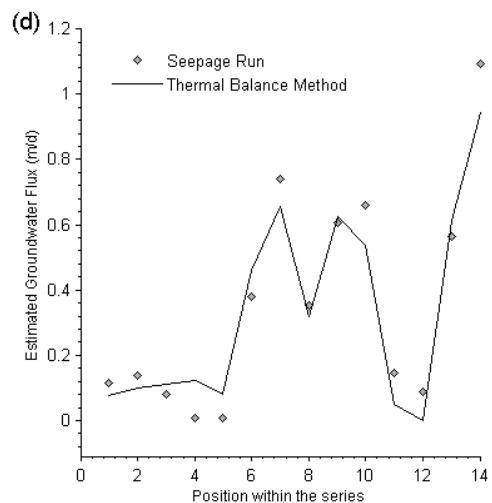
ACCEPTED



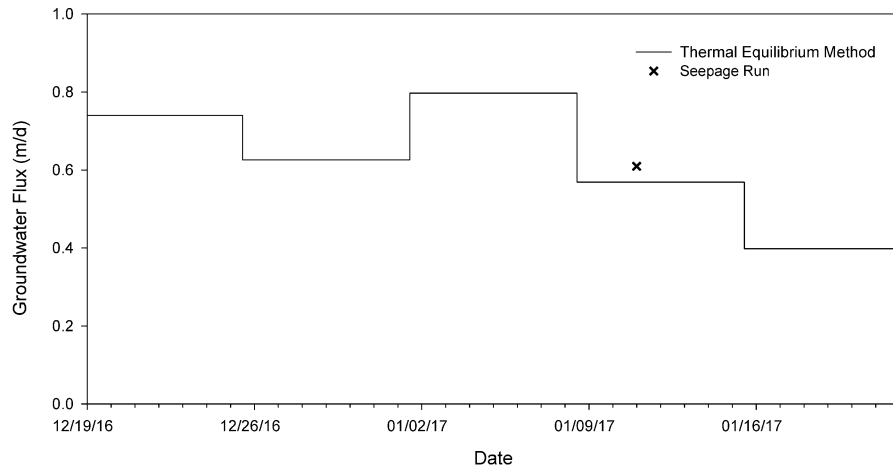
ACCEPTED MANUSCRIPT



(c) **GOODNESS-OF-FIT EVALUATION**  
 Evaluation of NSE: **VERY GOOD**  
 Probability of fit being:  
 - *Very good* (NSE = 0.900 - 1.000): 96.3%  
 - *Good* (NSE = 0.800 - 0.899): 3.7%  
 - *Acceptable* (NSE = 0.650 - 0.799): 0%  
 - *Unsatisfactory* (NSE < 0.650): 0% (p-value: 0)  
 Presence of outliers (Q-test): NO  
 Model bias: Underprediction by -5.7% of the mean  
 (NSE may be influenced by model bias)



ACCE



ACCEPTED

